

Research on Control Algorithm of Electric Linear Loading System

Jianjie Lei¹, Yuanxun Fan¹, Weidong Pan¹, Dejjia Tang², Jian Tao² and Zhiwei Xu²

¹*School of Mechanical and Electrical Engineering, Nanjing University of Science and Technology, NanJing, China*

²*Shanghai Aerospace Control Technology Institute, Shanghai, China*

Abstract. This paper mainly focused on the problems of low loading accuracy in electric linear loading system, Firstly, the mathematical model is done on loading motor, loading motor driver and ball screw in the system. Then, the current loop proportional control is introduced, which improves the response speed of the load motor; In order to improve the loading accuracy and restrain excess force, a parallel algorithm based on fuzzy PID and repetitive control is designed in the force loop. The fuzzy controller improves the dynamic performance and anti-interference ability of the system. The repetitive controller periodically adjusts the deviation, which reduces the steady-state error of the system. Combination of the two controller results in good dynamic and static characteristics. The simulation results show that the proposed control algorithm is feasible, which has a certain engineering reference value.

1 Introduction

Electric Linear Loading System (ELLS) is an important test device used to test the performance of linear servo. The successful development of ELLS can not only shorten the development cycle of the tested mechanism and reduce the development cost, but also improve test reliability and success rate. At present, most of the systems under study are electric rotary loading systems, that is, the loading of the rotary servos by the rotary electric machines, and the ELLS is mainly divided into the linear servomotors, the rotary servomotors with the ball screw. Considering the shortcomings in control difficulty and high cost of linear motor, this paper adopts the loading form of rotating motor with ball screw, but the nonlinear factors such as mechanical friction, gaps and servo position disturbance have some problems such as large excess force and signal hysteresis[1]. Therefore, on the basis of establishing the correct mathematical model of the system, how to improve the system's high response and high-precision control performance is the core issue of the study.

At present, domestic and foreign scholars have proposed a large number of control methods to improve the performance of ELLS. Ni[2] proposed a method based on dynamic fuzzy neural network to suppress the extra torque and improve the system response and tracking accuracy by combining with feedforward feedback and direct inverse control of the composite control strategy; Wang[3] proposed a nonlinear robust control algorithm of the electro-hydraulic load simulator, which address the actuator's disturbance and flow nonlinearity. Wang[4] proposed fuzzy adaptive torque control (Adaptive Fuzzy Torque Control, AFTC), which effectively restrain the

extra torque and improve the stability of the closed-loop system by using the small gain theorem. ND Manning[5] proposed a feedback linearization method which reduces and nearly eliminates the load dependence of the tracking response. R Ghazali[6] adopts a robust controller design using discrete-time sliding mode control, and a two-degree-of-freedom(2-DOF) is used to turn the DSMC, which reduce the phase lag trajectories and significantly show enhancement in tracking control performance.

The above literature, mainly from the servo motion compensation and anti-jamming controller design. Based on the linear servo high-precision mechanical properties testing, in order to overcome the mechanical nonlinear factors, steering disturbance and other issues, this paper proposes parallel structure which include fuzzy PID control and the repetitive controller. It not only improves the self-adaptive anti-jamming ability of the system, but also reduces the cumulative error in sinusoidal loading. The simulation results show that the composite control can significantly reduce the extra force and improve the loading accuracy.

2 System structure

ELLS is a position disturbance type torque servo system, which mainly consists of load motor, motor driver, real-time controller, sensor, multi-channel data acquisition card, and the rudder system constitutes a complete loading system.

As shown in Fig.1, the host computer PC sends a sine current signal through the EtherCAT communication protocol to control the output torque of the motor. The loading motor converts the rotational force into a linear

force through the ball screw to complete the linear load of the steering gear. The loading force is detected by high precision pressure sensor, the data acquisition card feedback to the controller, the formation of force closed-loop control to track load force command to complete the static and dynamic force loading.

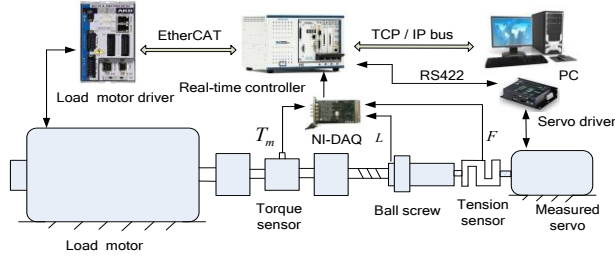


Figure 1. Electric linear load system structure

3 System mathematical model

The accuracy of the ELLS mathematical model largely determines the control performance of the system. Combined with this system, the model of the motor and the ball screw model are fully considered in the process of modeling. This paper assumes that the mechanical connection parts are both rigidly connected and ignoring the influence of the friction torque.

3.1 Load motor model

The load motor(PMSM) uses $i_d = 0$ control strategy. Under ideal conditions[7], the voltage balance equation and the electromagnetic torque equation can be written as:

$$\left. \begin{aligned} U_q &= R_a i_q + L_a di_q/dt + P\varphi_f W_m \\ J_a dW_m/dt &= T_e - T_L - B_a W_m \end{aligned} \right\} \quad (1)$$

The back EMF coefficient and electromagnetic torque are:

$$\left. \begin{aligned} K_e &= P\varphi_f \\ T_e &= P\varphi_f i_q \end{aligned} \right\} \quad (2)$$

In the above (1) and (2), where U_q is the voltage on q axis; R_a is the phase resistance of the motor stator; i_q is the current on q axis; L_a is the inductance on q axis; p is the motor rotor pole pairs; φ_f is the rotor permanent magnet flux; W_m is the motor output shaft mechanical angular velocity; T_e is the electromagnetic torque; T_L is the load torque; B_a is the motor friction coefficient; J_a is the motor's moment of inertia; K_e is the motor's back EMF coefficient.

3.2 Intermediate transformation model

Permanent magnet synchronous motor will rotate torque into linear force, and it needs to go through the ripple coupling, torque sensor and ball screw pair. These intermediate links should be taken into consideration because they have a certain impact on the accuracy of the system.

Torque sensor integrated error is $\pm 0.1\%$ FS, which meets the Hulk's law:

$$T_w = K_L(\theta_m - \theta_L) \quad (3)$$

so system torque balance equation is:

$$T_L = J_L d^2\theta_m/d^2t + B_L d\theta_m/dt + T_w \quad (4)$$

In the above(3) and (4), T_w is elastic torque; J_L is the load moment of inertia, which includes ball screw J_s and the coupling J_G , $J_L = J_s + J_G$; B_L is the equivalent load damping coefficient; K_L is the elastic stiffness coefficient; θ_m is the motor angular displacement; θ_L is the load angular displacement.

3.3 Torque and force relationship of ball screw

Rotating torque transforms into linear load force through the ball screw. The relation between output torque and linear relationship is:

$$F = T_L/r \tan \lambda \quad (5)$$

Linear servo run a distance L , then the corresponding angle of screw turned, displacement and angle are as follows:

$$\theta_L = 2\pi L/P \quad (6)$$

In the above (5) and (6), F is the linear load force; r is the ball screw radius; λ is the ball screw lead angle; P is the ball screw lead, L is the linear servo displacement.

When constructing the system model, the servo actuator, actuator and transmission mechanism are a closed system. Therefore, the actual displacement of the linear servo is approximated as the displacement command, and the displacement of the servo is regarded as a disturbance of the system.

Laplacian transformation of the above (1)-(6) can get the system control open loop control block diagram shown in Fig.2, where in the voltage control signal U_q is the input signal, the servo linear displacement, L is the disturbance signal, the straight line force F is the output signal.

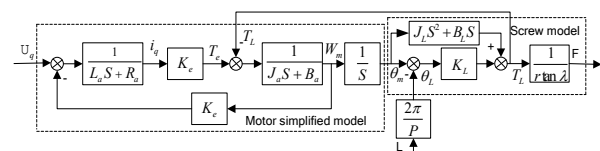


Figure 2. Controlled object control block diagram

4 Composite controller designer

4.1 Current loop design

During the servo failure test, the torque of the PMSM needs to be precisely controlled so that it can respond quickly. Therefore, the current is controlled by the

proportional control, and the control block diagram is shown in Fig.3.

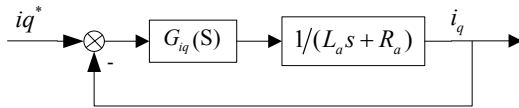


Figure3. Current loop control block diagram

Current open loop transfer function is:

$$G_k(S) = G_{iq}(S) / (L_a S + R_a) \quad (7)$$

The above (7) is the proportional coefficient of the current loop controller. It can be seen from the bode diagram of the system, and it is a stable system whose phase does not exceed -90° . The closed-loop transfer function of the system is as shown in (8), The current closed-loop transfer function consists of a first-order lag and a proportional.

$$G_c(S) = G_{iq}(S) / (L_a S + R_a + G_{iq}(S)) \quad (8)$$

Static deviation of the control system commonly uses $S=0$ closed-loop gain to evaluate. That is, the closer to 0 the gain is, the smaller the static deviation is. From (9), since the proportional gain is far greater than R_a , the gain is close to 0 and the static deviation of the system is small.

$$G_{iq}(0) = i_q(0) / i_q^*(0) = K_{iq} / (R_a + K_{iq}) \quad (9)$$

It can be seen from the frequency characteristics of the closed loop current loop in Fig.4 that the amplitude-frequency characteristics of the system are stable and are of a high bandwidth (3Khz), which shows fast current response and good dynamic and static characteristics.

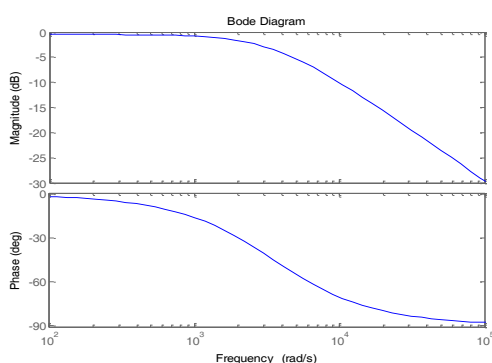


Figure.4 Current loop closed loop frequency

4.2 Force controller design

Considering the problems of large load steady-state error, phase lag and low response in the system, this paper uses the closed-loop feedback of output force and proposes the structure of parallel fuzzy PID and repetitive control. The block diagram of the concrete structure is shown in Fig.5.

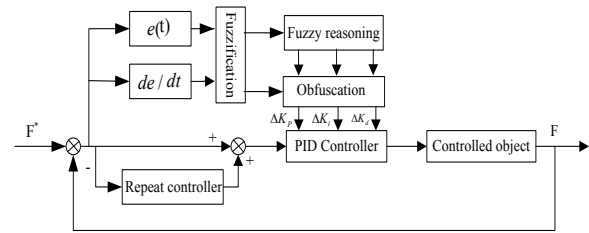


Figure5. Force composite control

4.2.1 Fuzzy PID Controller Design

a) Fuzzy PID structure

The fuzzy PID structure adopts the gain adjustment type. Because the controlled increment only relates to the error and the error rate of change sampling value, it has the advantages of saving the regulator memory and calculating the time[8]. Based on the premise of a stable system, the initial parameters of PID uses Z-N method of self-tuning: $K_{p0}=9$, $K_{i0}=1$, $K_{d0}=0.06$. The specific formula is:

$$\left. \begin{aligned} K_p(k) &= K_{p0} + \Delta K_p(k) \\ K_i(k) &= K_{i0} + \Delta K_i(k) \\ K_d(k) &= K_{d0} + \Delta K_d(k) \end{aligned} \right\} \quad (10)$$

b) Membership function and the fuzzy rules

For the fuzzy controller input error e , error rate of change ec and output $U (\Delta K_p, \Delta K_i, \Delta K_d)$, their fuzzy sets are as follows:

$$e, ec, U = \{NB, NM, NS, ZO, PS, PM, PB\} \quad (11)$$

For input and output linear scale transformation, the basic universe is $[x_{min}^*, x_{max}^*]$, the fuzzy universe of view is $[x_{min}, x_{max}]$, then $k = (x_{max} - x_{min}) / (x_{max}^* - x_{min}^*)$. The input deviation e and deviation of the rate of change ec fuzzy domain are defined as $(-6, -4, -2, 0, 2, 4, 6)$. The fuzzy universe of output variable U is $(-3, -2, -1, 0, 1, 2, 3)$. In actual application, the quantization factor (K_e, K_{ec}) and the scale factor (K_1, K_2, K_3) can be adjusted to map to the corresponding universe of discourse range. Membership functions adopt triangular functions with online calculations and occupy smaller systems.

Fuzzy rules are summed up after a lot of people's experiments and work experience [9]. The general rule of control rules are:

1. When the ELLS starts or stops running, the error e of the output force of the loading system becomes larger, so as to speed up the response of the system, K_p should be greater. To avoid the effect of differential saturation caused by the excessive e , K_d should be medium; To prevent loading system output force from greater overshoot, K_i should be zero.
2. When the ELLS is in normal operation, the error e

and the rate of change of error e are medium-sized, so as to reduce the overshoot of the system, properly take small K_p , K_i and take K_d appropriate values.

3. When ELLS outputs a constant force, e and ec should be small at this moment. In order to make the system stable, K_i and K_d should be increased appropriately. In order to avoid system oscillation in setting value and strengthen the anti-interference of the system, the reasonable value K_d should be taken.

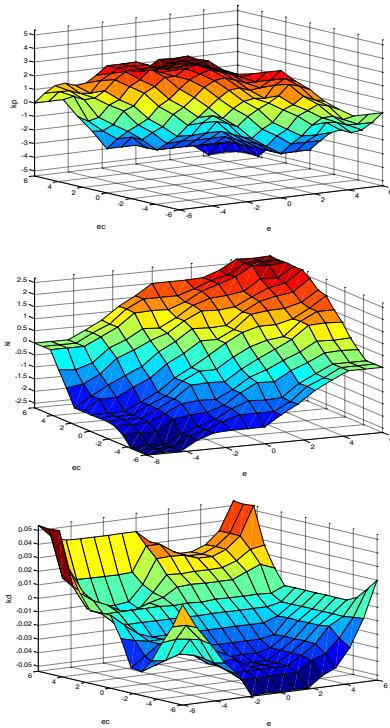


Figure 6. ΔK_p , ΔK_i , ΔK_d fuzzy rules surface

c) Obfuscate

After determining the fuzzy rules of the system, the output of the system adopts the weighted average method commonly used in industrial control, and takes each element $x_i (i=1,2,\dots,n)$ in the domain as the weighted coefficient $\mu(i)$ of the membership function of the fuzzy set output by the judgment, takes the product $x_i \mu(i)$, and then calculates The sum of the products $\sum_{i=1}^n x_i \mu(i)$, the average of the membership degree x_0 , and the final output of the system multiplied x_0 by the scaling factor to get the actual control volume.

$$x_0 = \frac{\sum_{i=1}^n x_i \mu(i)}{\sum_{i=1}^n \mu(i)} \quad (12)$$

4.2.2 Repetitive controller design

The repetitive control is based on the internal model principle and can be used to control the repetitive

trajectory of the servo system accurately. It can compensate the periodic signal and suppress the periodic disturbance of the load [10].

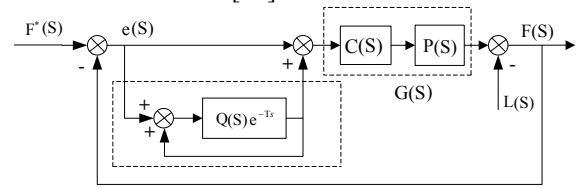


Figure7. Repetitive control system structure

a) System stability analysis

As can be seen from Fig.6, the relationship between the repetitive control system error $e(S)$ and the input signal $F^*(S)$ and the interference signal is:

$$e(S) = \frac{1-Q(S)e^{-TS}}{1-Q(S)e^{-TS}+P(S)} F^*(S) + \frac{1-Q(S)e^{-TS}}{1-Q(S)e^{-TS}+P(S)} L(S) \quad (13)$$

The (13) can be transformed into:

$$e(S) \Rightarrow \frac{1-Q(S)e^{-TS}}{1-[1-G_c(S)]Q(S)e^{-TS}} F^*(S) + \frac{1-Q(S)e^{-TS}}{1-[1-G_c(S)]Q(S)e^{-TS}} L(S) \quad (14)$$

In (13), $G(S) = P(S)$, $G_c(S) = G(S)/(1+G(S))$.

From (14), we get the system's characteristic equation:

$$1-[1-G_c(S)]Q(S)e^{-TS} = 0 \quad (15)$$

According to the stability criterion of classical control theory, all the eigenvalues of the system are in the left half of the S plane, so the system is stable.

b) Compensator design

Dynamic compensator $C(S)$ is designed to compensate for the amplitude and phase of the system to improve the system loading accuracy and stability. When $|1-C(S)P(S)| < 1$ converges to zero, the repetitive controller loading system converges fast and the external disturbance rejection capability of the system increases. However, $C(S)$ is impossible to approach the controlled object $P(S)$ in the entire frequency band. Considering repetitive amplitude attenuation and phase compensation in the high frequency range, Therefore, $C(S)$ with low-pass filter function, cycle delay compensation for the phase, so the design should meet the (16):

$$|1+C(S)P(S)| > 1 \quad (16)$$

c) Filter design

From Eq. (13), we can see that $1-Q(S)e^{-TS} = 0$ at that time, the error $e(S)$ of the system is close to zero. From Euler's formula $|e^{-TS}| = 1$, we can see that when $Q(S)$ is close to 1, the tracking capability is good, the steady-state error is small and the system is stable.

The selection of $Q(S)$ should ensure system stability and tracking accuracy, under the premise of

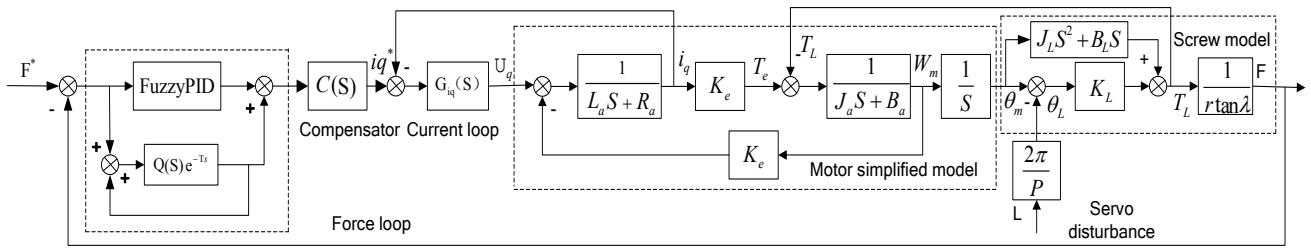


Figure8. Control system structure

$|Q(S) - Q(S)G_c(S)| < 1$, the actual signal often work in the low band, so $Q(S)$ usually choose low-pass filter, $Q(S) = 1/(\tau s + 1)$, when $s = j\omega$, low-pass filter frequency characteristics meet the following conditions:

$$\left. \begin{aligned} Q(j\omega) &\approx 1 \\ Q(j\omega) &< 1 \end{aligned} \right\} \quad (17)$$

On the basis of Fig.2, the current loop and the force loop are introduced into the system, therefore the block diagram of the control system is obtained and shown in Fig8.

5 System simulation

According to the control strategy of fuzzy PID and repetitive control presented in this paper, a system simulation model based on Matlab/Simulink is established. The system parameter table is shown in Table1:

Table1. System parameters

Parameters	Value	Parameters	Value
K_e	112V / Krpm	r	12.5mm
J_L	$9.2 \times 10^{-5} \text{ kgm}^2$	λ	17.6°
B_L	0.08Nm / Krpm	L_a	11.4mH
K_L	6500Nm / rad	R_m	2.1Ω
J_m	$9.1 \times 10^{-4} \text{ Kgm}^2$	τ	0.01
B_m	0.052Nm / Krpm	P	25mm
K_e	0.03	K_{ec}	0.01
K_1	1.2	K_2	1
K_3	1.5	K_{iq}	38

5.1 Linear load force tracking performance

Set sine load force command $F = 3000\sin(6\pi ft)$ as a system of incentives, compare traditional PID control and composite control load force tracking effect. Fig.9 is the PID control, there is a large deviation both in amplitude and phase, which can not meet the project "double ten indicators"; Fig.10 is a composite control tracking curve, the force command and output force curve basically coincide, greatly reducing the amplitude and phase deviation, the tracking performance of the system has also been greatly improved; Fig.11 is the load force error curve under two control mode, the amplitude of error

curve adopting composite control algorithm is decreasing as time goes by.

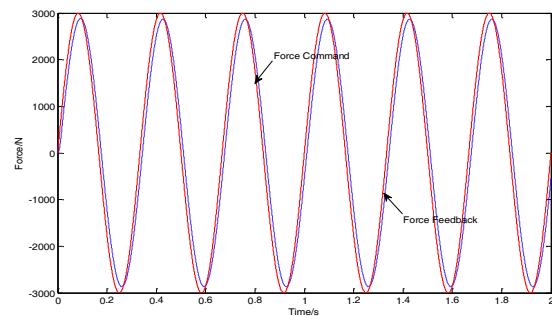


Figure 9. 3Hz/ PID control force tracking curve

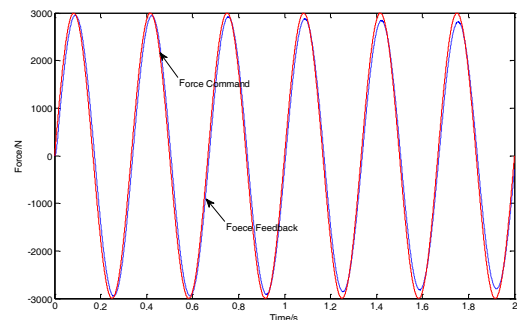


Figure10. 3Hz / Composite control force tracking curve

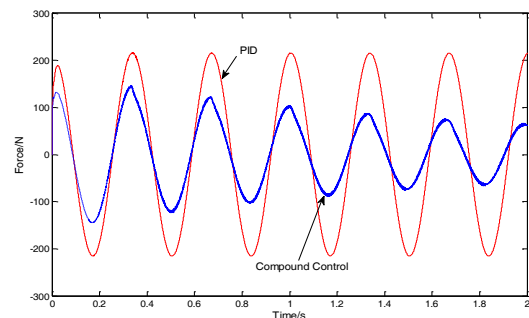


Figure11. Two kinds of control load force error curve

5.2 Excess force suppression ability

ELLS endures position coupling disturbance from active motion of actuation system, and this inherent is called excess force, So suppression of excess force is an important property for electric linear loading systems, and generally the commanding force is zero. The linear

actuator follows the specified sinusoidal path acted as the disturbance input. In order to compare the control effects under different controllers, traditional PID control and redundant force suppression simulation under compound control are carried out. Fig.12 shows that when the steering gear moves at 1mm/1Hz, the composite control compared with traditional PID extra force reduces from 150N to 60N. Fig.13 shows that when the steering gear moves at 1mm/3Hz, the composite control reduces 380N to 110N compared with the traditional PID, and as time goes by, the effect of restrain force is getting better and better.

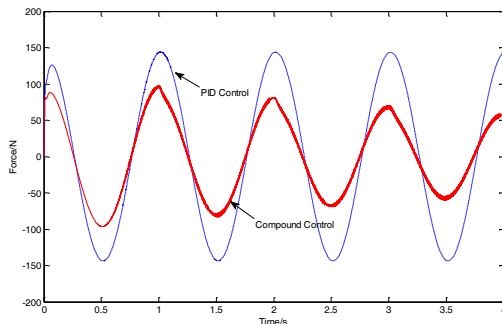


Figure12. 1mm/1Hz excess force suppress

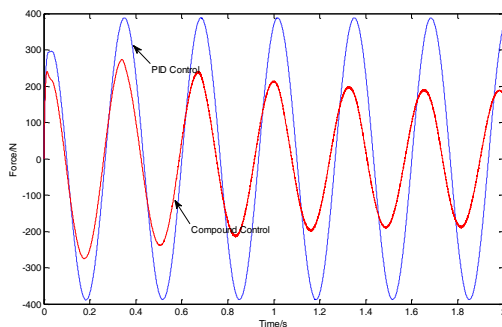


Figure13. 1mm/3Hz excess force suppress

6 Conclusion

ELLS is a key part in the design of electric load simulator. Compared with the torque servo system, ELLS has strong coupling and many nonlinear factors. In this paper, proposes a two-loop control structure of current loop and force loop closed-loop feedback. Current loop is

controlled by Proportional control, which improves the current response and steady-state error. The force loop uses the parallel method of fuzzy PID and repetitive control, which not only improves the accuracy of the loading force, but also reduces the steady-state error. The simulation shows that the control method is very good at tracking servo capability and suppressing excess force in low frequency.

References

1. Wang Chao, Hou Yuanlong, Wang Li, Influence analysis on electric load simulator for the gun control system. *Electric Machines and Control*,2015,**20** (12):73-81.
2. Ni Zhisheng, Wang Mingyan. A novel method for restraining the redundancy torque based on DFNN, *Journal of harbin institute of technology* ,2012,**44**(10):79-84.
3. Wang Chengwen, Jiao Zongxia, Wu Shun, etc. A practical nonlinear robust control approach of electro-hydraulic load simulator[J]. *Chinese Journal of Aeronautics*, 2014,**27**(3):735-744.
4. Wang Xingjian ,Wang Shaoping ,Zhao Pan. Adaptive Fuzzy Torque Control of Passive Torque Servo Systems Based on Theorem and Input-to-state Stability. *Chinese Journal of Aeronautics* ,2012,**25**(12):906-916.
5. ND Manring ,L Muhi, RC Fales ,etc. Using Feedback Linearization to Improve the Tracking Performance of a Linear Hydraulic-Actuator[J].*The American society of mechanical engineers*,2018,**1**(20): 1-6.
6. R. Ghazali, Y. M. Sam, M. F. Rahmat, etc. Discrete Sliding Mode Control for a Non-minimum Phase Electro-hydraulic Actuator System. *Asian Control Conference (ASCC)* ,2015:1-6.
7. Truong DQ, Ahn KK. Force control for hydraulic load simulator using self-tuning grey predictor-fuzzy PID. *Mechatronics*,2009,**19**(2):233-248.
8. Wang C W,Jiao Z X,Luo C J. An improved velocity synchronization control on electro-hydraulic load simulator. *Acta Aeronautica et Astronautica Sinica*, 2012, **33**(9): 1717-1725.
9. X.J.Wang, S.P.Wang,and X.D.Wang, Electrical Load Simulator Based On Velocity-Loop Compensation And Improved Fuzzy-PID ,*International Symposium on Industrial Electronics*,2009.
10. E Tung ,G Anwar ,M Tomizuka..Low Velocity Friction Compensation and Feedforward Solution based on Repetitive Control. *American Control Conference*. 2009,**115**(2): 2615-2620.